Research article

Changes in landscape composition and configuration in the Beressa watershed, Blue Nile basin of Ethiopian Highlands: historical and future exploration

Hamere Yohannes [a,b,*], Teshome Soromessa [b], Mekuria Argaw [b], Ashraf Dewan [c]

[a] Department of Natural Resources Management, College of Agriculture and Natural Resource Sciences, Debre Berhan University, P.O. Box: 445, Debre Berhan, Ethiopia
[b] Center for Environmental Sciences, College of Natural and Computational Sciences, Addis Ababa University, P.O. Box:1176, Addis Ababa, Ethiopia
[c] Spatial Sciences Discipline, School of Earth and Planetary Sciences, Curtin University, Perth, Australia

ABSTRACT

Analyzing long-term dynamics of landscape patterns can provide important insights into the changes in landscape functions, that are necessary for optimizing resource management strategies. This study primarily aimed at quantifying landscape structural change. The Land use/land cover (LULC) layers of 1972, 1987, 2002, and 2017 were mapped from Landsat images, and projected to 2032 and 2047. Factor analysis was then employed to select independent core metrics of landscape composition and configuration to characterize the landscape. A post-classification comparison indicated that, between 1972 and 2017, natural vegetation, grassland, barren land and waterbody covers declined by 89.9%, 67.9%, 67.8 and 15.9%, respectively. On the other hand, plantation increased by 692.1% followed by human settlement (138%) and farmland (21.8%). A similar trend is likely to continue in 2032 and 2047 with a slight decline in the plantation category in 2047. Analysis of landscape metrics revealed that between 1972 and 2017, the number of patches increased. Specifically, plantation, barren land, settlement and grassland increased by 171.4%, 69.7%, 65.8% and 28.6%, respectively. In contrast, natural vegetation, farmland and waterbody declined by 53.1%, 46.3% and 33.9%, respectively. Future predictions showed a declining trend of the number of patches for all LULC types. An increasing trend in the largest patch index and patch size for farmland, plantation, and settlement categories was observed across all years, suggesting intensified human activities in the landscape. Consequently, natural habitat category has declined and become fragmented. Landscape pattern has changed considerably and become more fragmented over the last 45 years. Nevertheless, the future projections suggest a decline in fragmentation and potentially increased assemblage of patches forming simple patterns with fewer number of large size class patches. The results of this study could perhaps be applied in designing strategies for landscape management planning and resource conservation decision-making.

1. Introduction

The notion of landscape is concerned with the interaction between spatial patterns and ecological processes (Mohamed et al., 2019). Landscape changes can lead to environmental modifications both at local and global scales (Rudel, 2009). For centuries, mankind has altered natural environment to meet their demand for resources (Berihun et al., 2019). Landscape dynamics is a complex part of land use, and landscape structural changes can be determined using land use/land cover (LULC) data (Vadjunec et al., 2018). LULC change detection is an important tool to identify geographical dynamics and its association with human activities.

However, it is often inadequate to provide detailed landscape structural properties such as composition and configuration (Dewan et al., 2012; Liu and Weng, 2013). Landscape structure is an indicator of spatial patterns of the ecosystem and connectedness between different landscape elements (Zhang et al., 2014). To understand landscape function and process, landscape structure and any structural changes are a prerequisite (Matsushita et al., 2006). Various landscape metrics have been developed to measure spatial patterns of landscape function and processes (McGarigal et al., 2012). Nagendra et al. (2004), highlighted the issue of integrating landscape patterns and LULC. Many other researchers have used this concept in different geographic settings (Dewan et al., 2012; Liu

and Weng, 2013; Nurwanda et al., 2016). In contrast, a handful of works integrated landscape metrics and LULC prediction tools such as Markov chain and Cellular Automata (CA-Markov) to assess changes in future landscape structure. Araya and Cabral (2010), modeled and analyzed urban land-use change using CA-Markov and landscape metrics in

Portugal. Dezhkam et al. (2017) and Yang et al. (2014) conducted similar studies in Iran and China, respectively.

Because of increasing human activities, environmental problem has become widespread in many parts of the world. The deterioration in environmental quality and widespread environmental degradation
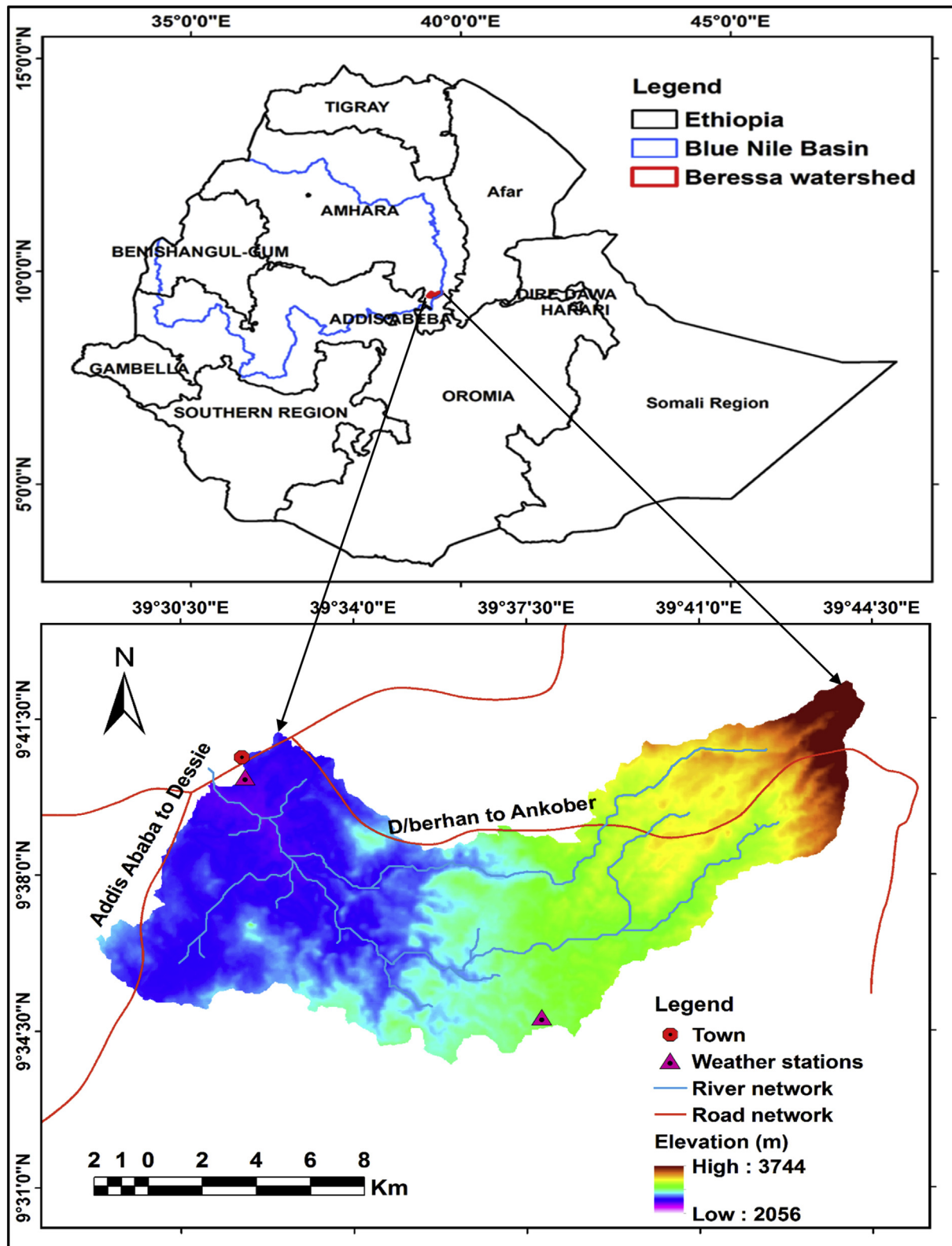
Figure 1. Location map, showing Beressa watershed in Amhara regional state, Ethiopia.

(biological and chemical) by air and water pollution (Basheer, 2017; Basheer and Ali, 2018; Burakova et al., 2018; Alharbi et al., 2018; Ali et al., 2005, 2015; Mohd and Khan, 2013; Alia and Alwarthan, 2017), and soil and vegetation loss can result in negative ecological and health consequences (Dunlap and Jorgenson, 2012). Ethiopia has been experiencing a range of environmental problems including deforestation, soil erosion, land degradation and fragmentation, and loss of biodiversity (Daley, 2015). Particularly, the central highland of Ethiopia, where this study was conducted, has been impacted by anthropogenic activities due to rapid population growth in the region. This has led to widespread resource loss, deforestation and expansion in agricultural practices (Amsalu et al., 2007; Kindu et al., 2013; Meshesha et al., 2016; Gashaw et al., 2017). Unregulated land use land cover changes coupled with poor land management practices are seriously undermining the country's natural resource stock, including the biodiversity and food production potential (Hamza and Iyela, 2012). Several studies have been undertaken to understand LULC changes in different parts of the Ethiopian Highlands (Kindu et al., 2013; Gashaw et al., 2017) including within the Beressa watershed (Amsalu et al., 2007; Meshesha et al., 2016). Almost all of these studies have reported extensive LULC change and illustrated complexity of the conversion process.

In general, studies on LULC change and landscape structure quantification in Ethiopia have not been well focused considering high variability in landscape of the country. A number of projects have looked at landscape structure and LULC change in the urban area of Mekelle city (Fenta et al., 2017), Jibat forest (Tolessa et al., 2016), South-West Ethiopia (Daye, 2012) and Holeta-Berga watershed (Gelet et al., 2010). These studies, however, were limited in scope and have not really examined future trends in landscape pattern change despite the fact that changes in landscape pattern can have serious implications in ecological functioning. It is evident that there is currently a real lack of detailed information and data regarding landscape structural change in this region. This study is designed to fill this gap by evaluating past and projected LULC trends, and quantifying landscape structure.

2. Material and methods

2.1. The study area

The study area is the Beressa watershed (centered on 39°29′ - 39°44′ E longitude and 9°34′- 9°42′ N latitude) which is situated approximately 130 km northeast of Addis Ababa, the capital of Ethiopia (Figure 1). It has an area of 21367.26 ha and is characterized by mountainous and hilly topography, with elevations ranging from 2056 to 3744 m above sea level (m a.s.l). It spans the Basona Werana and Angolelana Tera districts, in the North Shewa Zone of Amhara Regional State, Ethiopia. This area is an intensely cultivated part of the Ethiopia northern central highland's crop belt. The Beressa river, a major perennial waterway, flows in a north-westerly direction pass the Debre Berhan township to the Jemma River, a tributary of the Blue Nile basin.

The mean monthly temperature of the watershed area ranges from 2.8 to 21.9 °C with a mean of 13.18 °C. Mean annual rainfall ranges from 698.5 to 1083.5 mm with a mean annual total of 920 mm (EMA (Ethiopia Meteorology Agency), 2017) (Figure 2).

The major soil types of the watershed comprise Cambisols, Vertisols, Regosols and Luvisols, with very few Leptosols (MoWIE, 2017). Rainfed agriculture is the main source of livelihood for majority of the population. This sector is characterized by smallholder mixed crop-livestock farming. Commonly cultivated crops include wheat (*Triticum aestivum* L.), Barley (*Hordeum vulgare* L), horse bean (*Vicia faba* L.), field pea (*Pisum sativum* L.), Lentil (*Lens culinaris* L.), Teff (*Eragratis teff*), linseed (*Linum usitatissimum* L.) and chick peas (*Cicer arietinum* L.). Cattle and sheep production are also practiced in the study area.

2.2. Data acquisition, image preprocessing and classification

Landsat images, comprising 1972_MSS, 1987_TM, 2002_TM and 2017_OLI/TIRS, (path 167, row 53) were obtained from USGS (http://earthexplorer.usgs.gov). They were used to derive multitemporal data of the study area. The images retrieved represent dry season when spectral differences between the various land cover types are greatest and cloud contamination is minimal. Digital elevation model (DEM) from ASTER GDEM at 30m was also obtained from http://dwtkns.com.srtm. Infrastructural information such as roads and towns were acquired from Ethiopia Ministry of Water Irrigation and Electricity (MoWIE, 2017). The river network map was generated in Arc SWAT 2012.10.3.18 (https://swat.tamu.edu/software/arcswat/).

Geometric, radiometric and atmospheric corrections were conducted and digital number (DN) were converted to Top-of-Atmosphere (ToA) reflectance values using the DOS1 atmospheric correction tool (Congedo, 2016). The 1972 image was resampled to 30m using the nearest neighbor resampling method to align with the pixel size of other Landsat sensors (Kumar et al., 2018). A supervised classification was employed using maximum likelihood classification (MLC) algorithm. Spectrally
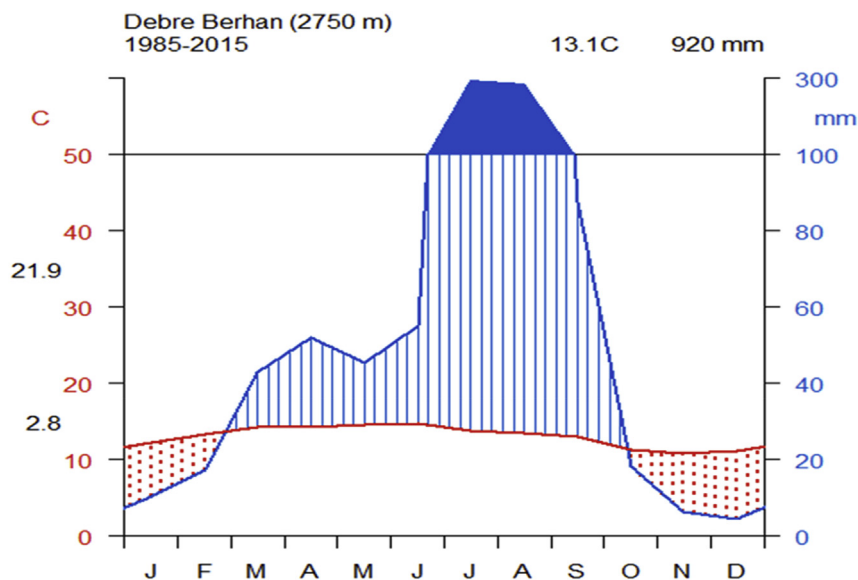
Figure 2. Rainfall and temperature distribution of Beressa watershed.

homogeneous areas were defined as training pixels using a region-growing algorithm (Macchi and Tiepolo, 2014). Post-classification smoothing was used to remove the salt-and-pepper effects (Lillesand and Kiefer, 1999). Sieving was then applied to the classified LULC to recode any isolated pixels. Finally, seven LULC categories were defined for the study area (Table 1). A cross tabulation was performed to determine conversion of one LULC category to another. A temporal comparison of values provides statistics for each period (Gashaw et al., 2017; Berihun et al., 2019). The following equations were used:

$$Percent\ of\ change(\Delta\%) = \frac{Area_{final\ year} - Area_{initial\ year}}{Area_{initial\ year}}\ x\ 100 \tag{1}$$

where, area is the extent of each LULC type; positive values suggest a gain while negative values represent a loss.

$$Rate\ of\ change(ha\ /\ year) = \frac{Area_{final\ year} - Area_{initial\ year}}{N} \tag{2}$$

where, N is the time interval between initial and final years.

2.3. Accuracy assessment

Ground control points (GCPs) were collected from a variety of sources, including field visits, Google Earth and vegetation maps (Rujoiu-Mare and Mihai, 2016). They were used as reference data to evaluate the results. A total of 390 samples (a minimum of 50 per class), following Congalton & Green (2009), were collected using a random sampling method. A comparison between the classified images and available ground truth information was conducted using the kappa index of agreement (KIA) and the quantity and allocation disagreement technique (Pontius and Millones, 2011). User's accuracy, producer's accuracy, kappa coefficient, overall accuracy and quantity disagreement and allocation disagreement (Table 2) were computed for each period. A kappa value > 0.8, indicated strong to perfect agreement with high reliability Singh et al., 2015

2.4. Land use/land cover change prediction

Spatially dynamic Cellular Automata-Markov chain (CA-Markov) model was used to predict future LULC for the years 2032 and 2047. The CA-Markov model (comprising a cellular state, cellular space, cellular neighborhood and transition rules), is expressed as (Chu et al., 2018):

$$S_{(t+1)} = (f(S_{(t)},\ N) \tag{3}$$

where, S is the set of finite and discrete cellular states, *t* and *t+1* represent different moment in time, N is cellular neighborhood, and *f* is cellular transition rules in local space.

The initial calibration utilized 2002 LULC map and Markov transition area of 1987 and 2002 to simulate 2017 LULC map. Simulation of future LULC maps was conducted following a check of initial calibration accuracy, essentially comparing simulated map of 2017 with the actual map.

Cross tabulation was employed to estimate KIA and quantity-allocation disagreements (Pontius and Millones, 2011).

Transition probability areas from the years 2002 and 2017, a classified LULC map of 2017, and a set of transition suitability images were then used to predict LULC patterns for two years, i.e., 2032 and 2047. The relative suitability area for each LULC was identified using factors and constraints defined by Eastman (2012) (Table 3).

2.5. Computation and selection of landscape metrics

To understand composition and configuration of the watershed at the class level, FRAGSTATS (v. 4.2.1) was used (McGarigal et al., 2012). It calculates a large set of landscape metrics for an area into elements such as patch density, shape, core area, diversity, contagion, and interspersion (Dewan et al., 2012). Many landscape metrics can be used to analyze spatial patterns of landscape, and many of the indices are highly correlated with each other (Apan et al., 2002). In this study, ecologically important landscape metrices are selected based on the aim of this study (Cushman et al., 2008).

Principal Component Analysis (PCA) was used for factor extraction. Important metrics were selected using an evaluation of the degree of redundancy based on a correlation matrix (Riitters et al., 1995). Factors are subjected to varimax rotation to determine loading factors, and components that have an eigenvalue of >1 are retained (Weide and Beauducel, 2019). Following data normality test, Spearman's product moment correlation between selected landscape metrics is used. The metrics that show an average in-group correlation of >0.8 are considered redundant (Cat Tuong et al., 2019). Only one of the metrics is retained for further analysis based on its ecological relevance. Five important landscape metrics: area metrics (LPI and MPS), shape metrics (AWMPFD) and aggregation metrics (AI and NP), are selected to characterize landscape composition and configuration in the Beressa watershed (Table 4). An analysis was performed using the R (v.3.6.2) software package (R Core Team, 2019).

3. Results and discussion

3.1. Land use/land cover changes between 1972 and 2017

LULC changes were categorized into four epochs, 1972–1987, 1987–2002, 2002–2017 and for the entire period, 1972 to 2017. The spatio-temporal distribution of each LULC category is presented in Figure 3, and an analysis of the extent of each LULC type is shown in Figure 4. When comparing the first period with successive periods, it is evident that the rate of change in waterbody, barren land, grassland and natural vegetation is lowest in this first period, and expansion of farmland is highest. The change however varied due to continuous shrinkage of natural vegetation, grassland, barren land and waterbody categories in response to an increase in settlement and plantation categories in the following two periods (Table 5, Figure 4). Farmland is the dominant LULC in the study periods and currently more than two thirds of the total area is under cultivation. This cover type has increased on an average 57.5 ha per year over the study period (Figure 3; Table 5). Analysis

Table 1. Description of different land use/land cover classes of the Beressa watershed.

LULC	Description
Natural vegetation (NV)	Comprises mixed indigenous trees and shrubs in natural forest, woodland and shrub land including *Junipers procera, Hagenia abyssinica* and *Acacia abyssinica.*
Plantation (PL)	Trees planted around homesteads and on degraded lands, dominantly *Eucalyptus*
Grassland (GL)	Grass cover, forbs and pasture land with no pattern
Settlement (ST)	Rural and urban settlements including villages, scattered houses, buildings, roads, industries and institutions etc.
Barren land (BL)	Land with little or no vegetation, exposed rocks and gullies
Farmland (FL)	Cultivated land, dominantly used for annual crops and fallow land
Waterbody (WB)	Includes rivers, streams, and pond water

Table 2. Accuracy assessment of 1972, 1987, 2002 and 2017 classified images.

LULC	1972		1987		2002		2017	
	PA	UA	PA	UA	PA	UA	PA	UA
Barren land	86	84.3	88	84.6	88	88	82	93.2
Farmland	90	88.2	92	92	94	90.4	98	77.8
Grassland	86	86	88	89.8	96	85.7	94	95.9
Natural vegetation	90	93.8	92	93.9	88	95.7	92	100
plantation	86	89.6	90	90	94	90.4	96	92.3
Settlement	90	91.8	92	93.9	90	97.8	94	100
Waterbody	96	94.1	98	96.1	96	100	98	100
Overall Accuracy (%)	89.66		91.43		92.29		93.42	
Kappa coefficient	0.88		0.90		0.91		0.92	
AD (%)	8.18		7. 96		7.7		6.5	
QD (%)	1.73		1.55		0.6		0.4	

PA: producer's accuracy, UA: user's accuracy, AD: allocation disagreement, QD: quantity disagreement.

Table 3. Factors and constraints and their weights used for predicting LULC.

LULC	Factors	Constraints	Criteria weight	Consistency ratio
Natural vegetation	Natural vegetation		0.53	0.01
	Distance to road		0.16	
		Distance to settlement	0.31	
Plantation	Plantation	None	0.18	0.04
	Natural vegetation		0.15	
	Grassland		0.16	
	Settlement		0.13	
	Farmland		0.14	
	Barren land		0.15	
	Waterbody		0.09	
Grassland	Grassland area	None	0.34	0.01
	Distance to settlement		0.23	
	Distance to road		0.21	
	Distance to river		0.08	
	elevation		0.14	
Settlement	Settlement area		0.4	0.05
	Distance to town		0.27	
	Distance to road		0.11	
	elevation		0.1	
		Slope (>5%)	0.12	
Barren land	Barren land area		0.43	0.04
	Farmland		0.14	
	Plantation		0.13	
	Grassland		0.1	
	Natural vegetation		0.13	
		Settlement	0.06	
		Water body	0.01	
Farmland	Cultivated land		0.38	0.02
	Distance to river		0.2	
	Distance to road		0.17	
	Distance to settlement		0.01	
	Elevation		0.08	
		Slope (>10%)	0.16	
Waterbody	Waterbody area		0.61	0.03
		Natural vegetation	0.22	
		Plantation	0.02	
		Grassland	0.03	
		Settlement	0.01	
		Farmland	0.02	
		Barren land	0.09	

Table 4. Description of landscape metrics used in this study.

Acronym	Metrics*	Description (unit)	Indicators
LPI	Large Patch Index	Percentage of landscape composed of the largest patch (%)	Dominance
MPS	Mean Patch size	Average size of the patch comprising each class (ha)	Fragmentation
AWMPFD	Area weighted mean Patch Fractal Dimension	Measures aspects of patches on the basis of fractal geometry (none)	Shape complexity
NP	Number of Patches	Total number of patches in the landscape of a particular class (none)	Fragmentation
AI	Aggregate Index	Percentage of a neighboring pixel of the same LULC class (%)	Aggregation

* McGarigal et al. (2012).
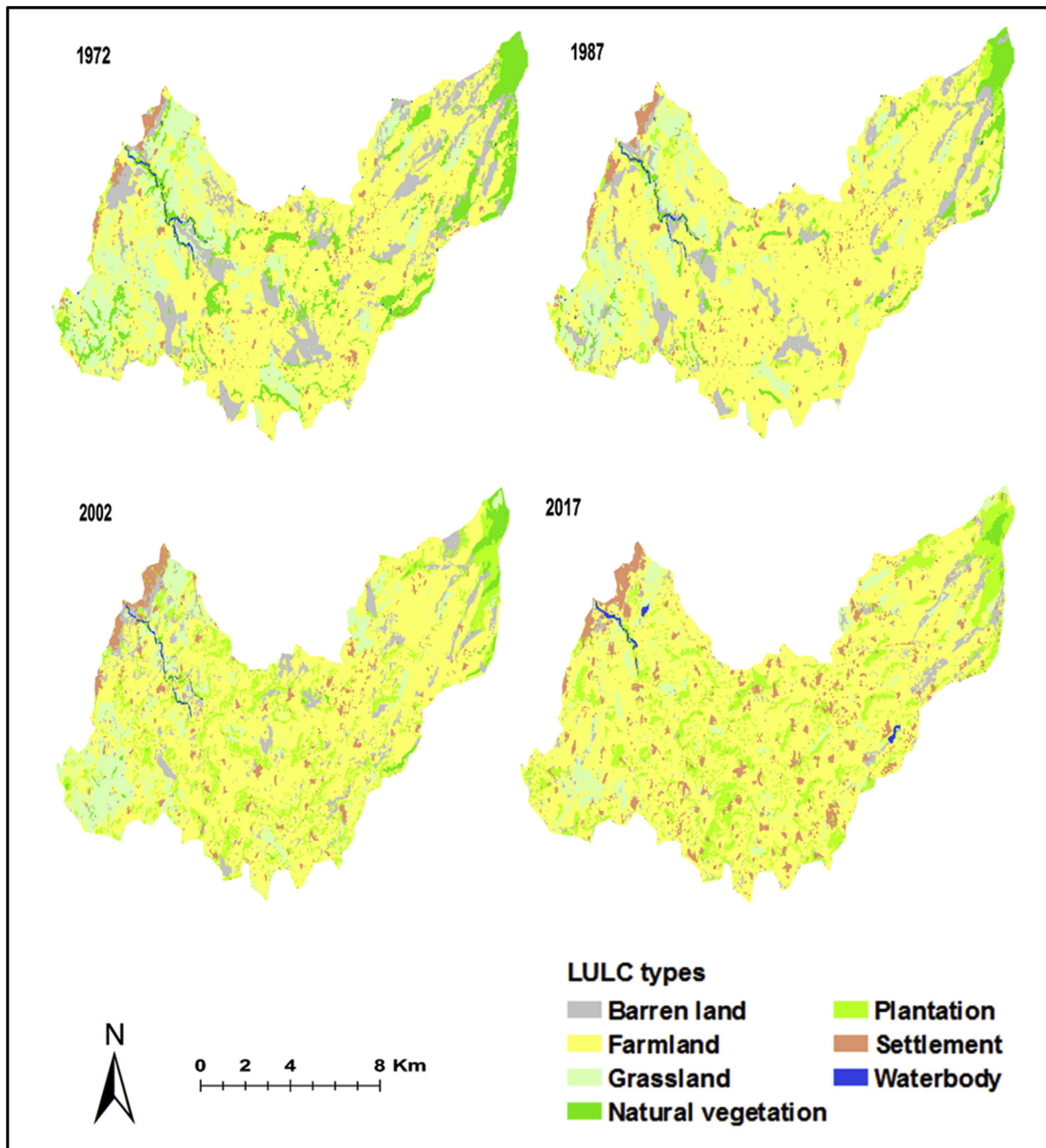
Figure 3. LULC maps of the Beressa watershed for 1972, 1987, 2002 and 2017.
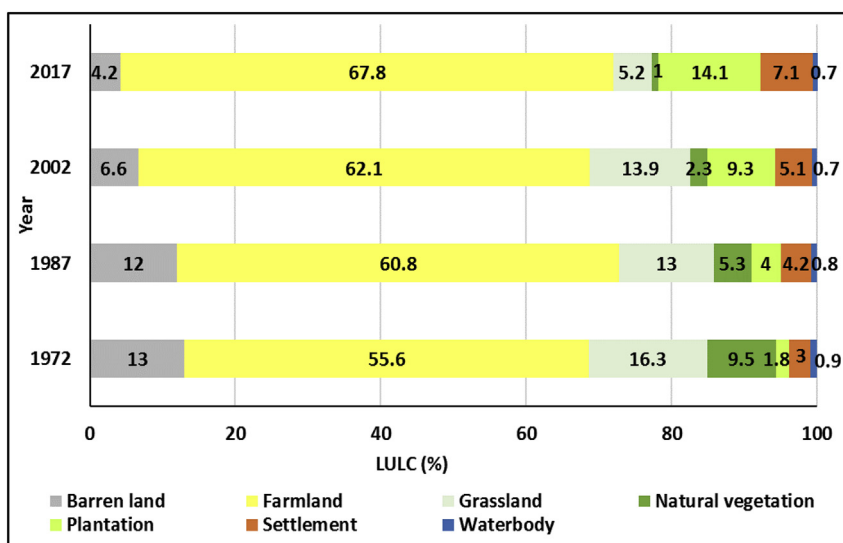
Figure 4. Area coverage of LULC for 1972, 1987, 2002 and 2017.

Table 5. Changes in LULC between 1972 and 2017.

LULC*	Percent change (%)				Annual rate of change (ha year^{-1})			
	1972–1987	1987–2002	2002–2017	1972–2017	1972–1987	1987–2002	2002–2017	1972–2017
BL	-8.2	-44.5	-36.7	-67.8	-15.2	-75.9	-34.7	-41.9
FL	9.4	2.1	9	21.8	74.3	18.2	79.9	57.5
GL	-20	6.5	-62.3	-67.9	-46.4	12	-122.9	-52.4
NV	-44.5	-55.6	-59.2	-89.9	-60	-41.5	-19.7	-40.4
PL	125.2	132.8	51.1	692.1	31.6	75.6	67.7	58.3
ST	38.8	22.4	40.1	138	16.5	13.3	29.1	19.6
WB	-7.6	-14.5	6.4	-15.9	-0.9	-1.7	0.6	-0.7

* refer Table 1 for LULC definition.

further shows that grassland was the second-largest LULC class until 2002 but were replaced by plantation cover during 2017 (Figure 4).

Significant areal expansion is observed in plantation (692.1%) and settlement (138%) covers during the study period. At the same time, the amount of natural vegetation, grassland, barren land, and waterbody LULC reduced to 89.9%, 67.9%, 67.8%, and 15.9%, respectively (Table 5).

The fluctuations in LULC change observed during the study period are undoubtedly associated with rapid population growth. A decline in soil fertility, resulting from intensive farming, has also forced farmers to expand their activities and move to steeper terrain and onto more marginal lands. Difficult to obtain energy sources such as wood (fuel for cooking and for house construction), land reallocation for cultivation and settlement (especially for the younger generation and retired military personnel) appeared to have influenced this phenomenon. This observation aligns with other studies which have been conducted in the Blue Nile basin of Ethiopian highlands and elsewhere (Amsalu et al., 2007; Meshesha et al., 2016; Gashaw et al., 2017; Yesuph and Dagnew, 2019; Hassan et al., 2016; Munthali et al., 2019; Jayne et al., 2014). The expansion of plantation (consisting of mainly *Eucalyptus* species) in the watershed area resulted in low productivity of cultivated lands due to depletion of important soil nutrients. The economic importance of *Eucalyptus* plantation is increased due to its market demand and fast-growing nature. Farmers have therefore attempted to diversify the type of farming being undertaken in order to increase their income (Minta et al., 2018). An alteration of natural vegetation systems has also been observed in the study area. This is due to expansion of the amount of land under cultivation and increasing demand for household fuelwood (including charcoal production), a direct result of population pressure leading to loss of biodiversity. The results of this study accord with the observations of Yesuph and Dagnew (2019), who reported that loss of vegetation is associated with loss of wildlife habitat causing widespread habitat fragmentation and a reduction in wildlife species. Population numbers in the region increased exponentially where the watershed is located (Figure 5). As a result, expansion of plantation, settlement and farmland are widespread, leading to a significant decline in natural vegetation, grassland, barren land and waterbody (Table 5).

The LULC class transition flagged notable changes in land use/cover during the study period (Table 6). A total of 3759 ha of land experienced a transition from one land class to another, (17.6% change during the first period), 8057 ha (37.7% change during the second period) and 7729 ha (36.1% change during the third period). According to transition matrix assessment, the highest rate of conversion was recorded in regards barren land (47.6%), waterbody (47.3%) and grassland (45%) which converted to farmland. Settlement to grassland was the lowest area conversion observed (Table 6). Among LULC classes, farmland was found to be little effected (about 80% remaining unchanged). An analysis of net gains and losses for each LULC class shows that grassland experienced significant loss (624.0 ha), followed by natural vegetation (392.7 ha). On the contrary, substantial gains are observed in settlement (723.2 ha), farmland (295.3 ha) and plantation (257.4 ha) land covers (Table 6).
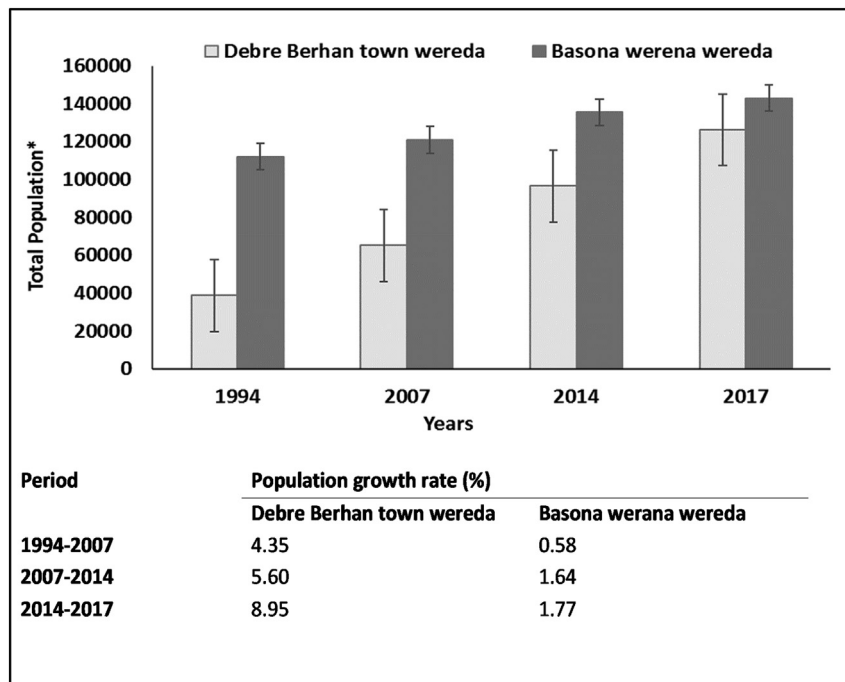
Figure 5. Total population and population growth rate (1994–2017) *source = Ethiopian Central Statistical Authority (CSA).

Table 6. Transition area matrix between 1972 and 2017.

LULC	unit	BL	FL	GL	NV	PL	ST	WB	Total	Loss	Net change
BL	ha	93.4	655.5	89.8	0	359.2	179.6	0	1377.5	1284.1	-119.3
	%	6.8	47.6	6.5	0	26.1	13	0	100		
FL	ha	504.8	10124.9	793.7	0	723.2	853.4	0	13000	2875.1	295.4
	%	3.9	77.9	6	0	5.6	6.6	0	100		
GL	ha	122.9	916.4	167.1	0	592.3	223.5	0	2022.2	1855.1	-624.0
	%	6	45.3	8.3	0	29.3	11.1	0	100		
NV	ha	61	126.2	18.3	8.8	122.1	65.1	0	401.5	392.7	-392.7
	%	15.2	31.4	4.6	2.2	30.4	16.2	0	100		
PL	ha	312.4	600.8	295.3	0	772	450.6	68.8	2499.9	1727.9	257.3
	%	12.5	24	11.8	0	30.9	18	2.8	100		
ST	ha	140.2	761.7	18.3	0	152.3	761.7	0	1834.2	1072.5	723.2
	%	7.6	41.6	1	0	8.3	41.5	0	100		
WB	ha	23.5	109.9	15.7	0	36.1	23.5	23.7	232.4	208.7	-139.9
	%	10.1	47.3	6.8	0	15.5	10.1	10.2	100		
Total (ha)		1258.2	13295.4	1398.2	8.8	2757.2	2557.4	92.5			
Gain (ha)		1164.8	3170.5	1231.1	0	1985.2	1795.7	68.8			

3.2. Prediction of land use/land cover change

3.2.1. Validation of CA-Markov model

Figure 6 shows actual versus simulated LULC for 2017. A comparison of the maps shows good agreement in terms of quantity-allocation agreement/disagreements and kappa statistics. Strong agreement between actual and simulated LULC maps shows the following, chance agreement (24%), quantity agreement (48%), allocation agreement (62%), allocation disagreement (10%), quantity disagreement (0.06%), kappa for no ability (Kno) (89.1%), Klocation (88.2%), Klocationstrata (88.2%) and Kstandard (83.7%). These metrics indicate good performance of the model in simulating future LULC and the variation between classified and simulated maps was minimal for all LULC categories (Figure 6). The results indicate that CA-Markov modelling can is a reliable predictor of future LULC in the study area. Studies by Gashaw et al. (2017); Mohamed and Worku (2020) and Palmate et al. (2017) have also

reported good agreement between simulated and classified LULC maps therefore confirming the model's robustness in predicting future LULC changes, both in Ethiopia and elsewhere.

3.2.2. Future land use/land cover change

During the two projected periods (2017–2032 and 2032–2047), farmland is expected to increase, followed by both plantation and settlement (Figure 7). The same trend would be expected to continue during the future, although loss and gain statistics between LULC categories may vary depending on the degree of human activities. Nevertheless, the rate of overall change is expected to be less than in the earlier periods. However, general trend of LULC changes in the Beressa watershed shows that the changes experienced in the recent past are likely to continue into the future. The predicted LULC change analysis shows that grassland, barren land, natural vegetation and waterbody categories could decrease, while areas of settlement, farmland, and plantation might increase
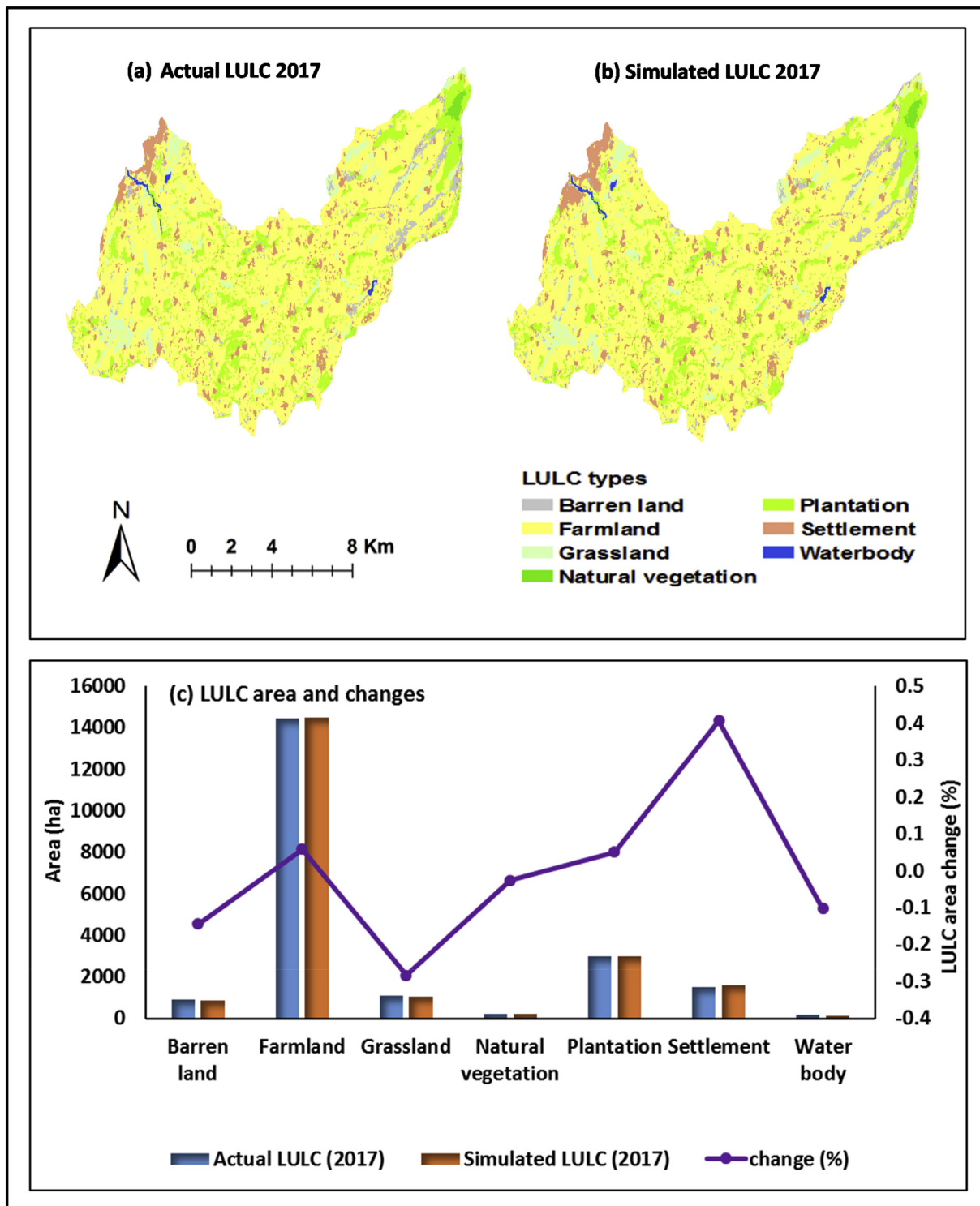
Figure 6. Comparison of simulated versus actual LULC maps, 2017

(Figure 8; Table 7). A slight decline in the plantation category in 2047 is also noticed.

The greatest decline is projected for natural vegetation and water-body (99.47% and 73%), with an annual projected loss of 6.7 and 3.8 ha, per respectively from 2017 to 2047. The total decline of these classes has the potential to be much higher than it was in the past. In contrast to this, the rate of decline for grassland (60.9%) and barren land (54.56%) could be lower than predicted. Settlement, farmland, and plantation could in-crease by 37.65%, 5.39% and 4.5% (Table 7). The reduction of valuable

natural land covers and expansion in human-dominated land-use activities strongly suggest that human disturbance will undoubtedly continue to affect future landscape functionality. A study by Gashaw et al. (2017), in the Andassa watershed, Blue Nile basin showed that areas under cultivation, and those impacted by urban developments, would change at a lower rate in the future compared to the past. The ongoing expansion of human settlement affects both ecosystem functionality and landscape stability through a reduction in water and sediment retention and the loss of local biodiversity and regional climatic regulation. Similarly, an
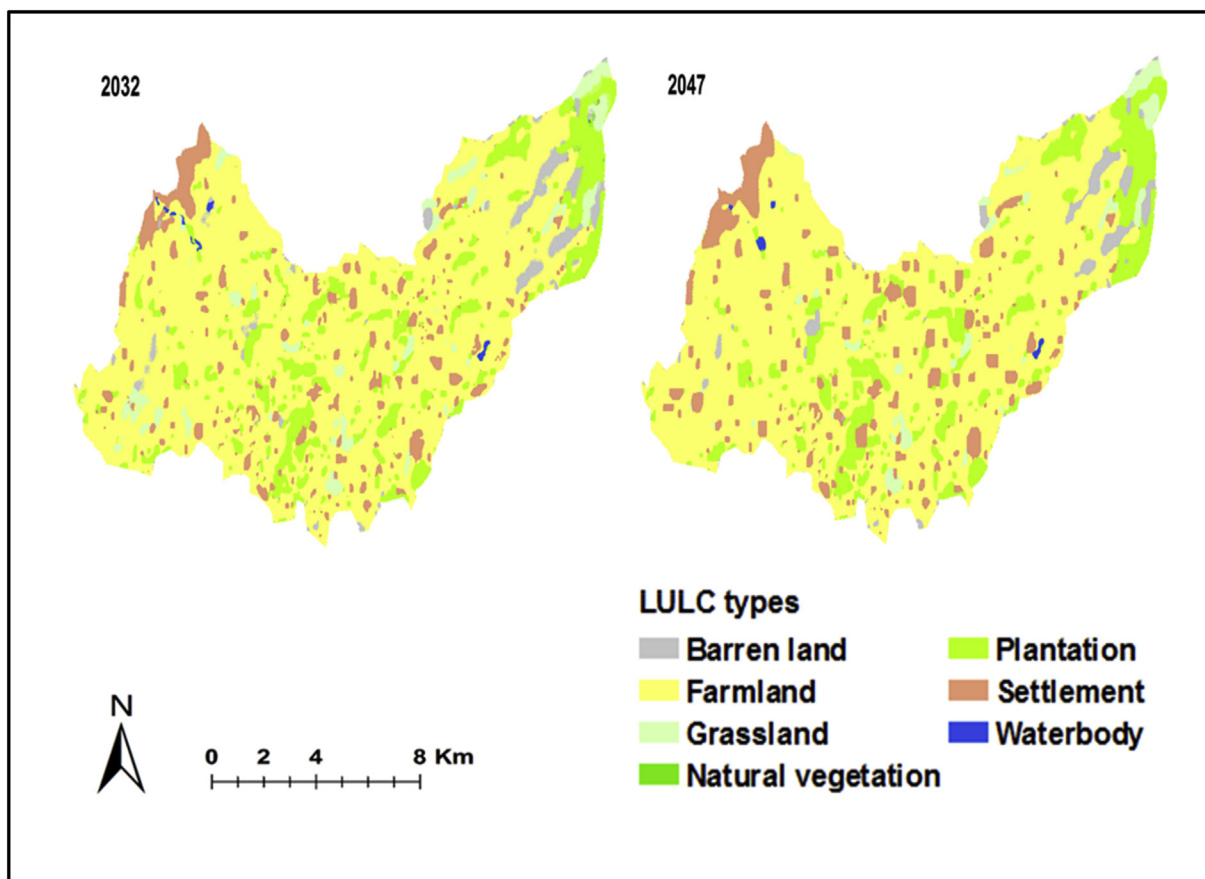
Figure 7. Simulated LULC maps of the Beressa watershed for 2032 and 2047.
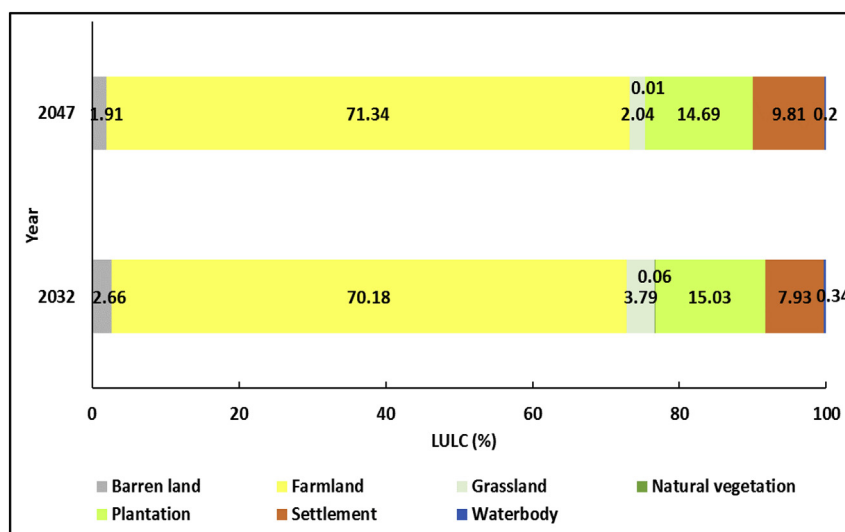
Figure 8. Area of projected LULC (2032 and 2047).

increase in the amount of area under cultivation can weaken the functionality, stability and biodiversity of ecosystems, as well as negatively impacting water regimes, soil quality and erosion rates (Prokopov et al., 2019). The popularity and associated rate of expansion of plantation areas (particularly those consisting of E*ucalyptus* species), is high in Ethiopia. This adversely affects the region's hydrological balance, leading to a depletion in soil nutrients, loss of soil and biodiversity, all of which impact functionality of an ecosystem (Minta et al., 2018). The change of

important natural land covers alters natural habitats composition and configuration could therefore threaten ecological stability (Prokopov et al., 2019).

Table 8 shows potential areal changes from one LULC class to another for the period 2017 to 2047. The main conversions are expected to occur from natural vegetation into grassland and plantation, grassland into farmland and barren land, barren land into farmland, plantation and settlement, and waterbody areas into farmland, plantation and grassland.

Table 7. Changes in LULC for 2032 and 2047.

LULC	Area change (%)			Annual change rate (ha yr^{-1})		
	2017–2032	2032–2047	2017–2047	2017–2032	2032–2047	2017–2047
BL	-36.60	-28.25	-54.51	-21.91	-10.72	-16.32
FL	3.68	1.65	5.39	35.48	16.46	25.97
GL	-27.47	-46.21	-60.99	-20.46	-24.97	-22.72
NV	-93.76	-91.69	-99.47	-12.72	-0.77	-6.75
PL	6.90	-2.25	4.5	13.82	-4.80	4.51
ST	11.20	23.77	37.65	11.40	26.84	19.12
WB	-53.67	-41.83	-73.05	-5.61	-2.03	-3.82

Table 8. Transition area matrix of the projected LULC (2017–2047).

LULC	unit	BL	FL	GL	NV	PL	ST	WB	Total	Loss	Net change
BL	ha	333.8	315.6	21.5	0	87.4	89.8	0	848	514.2	-76.4
	%	39.4	37.2	2.5	0	10.3	10.6	0	100		
FL	ha	322.5	13296.9	79.6	0	726.1	258.9	0	14684	1387.1	91.2
	%	2.2	90.6	0.5	0	4.9	1.8	0	100		
GL	ha	41.8	438.6	410	0	20.1	47.0	0	957.6	547.6	-417.4
	%	4.4	45.8	42.8	0	2.1	4.9	0	100		
NV	ha	5.7	0	21.2	20.4	150.5	5.6	0	203.5	183.0	-183
	%	2.8	0	10.4	10	74.0	2.8	0	100		
PL	ha	51.7	516.4	0.3	0	2360.7	98.2	0	3027.2	666.5	367.3
	%	1.7	17.1	0	0	78.0	3.2	0	100		
ST	ha	14.8	182.8	5.5	0	44.0	1336.9	0	1584	247.1	256.3
	%	0.9	11.5	0.3	0	2.8	84.4	0	100		
WB	ha	1.3	25.0	2.2	0	5.7	3.8	24.7	62.8	38.1	-38.1
	%	2.1	39.8	3.5	0	9.2	6.1	39.3	100		
Total (ha)		771.6	14775.2	540.2	20.4	3394.6	1840.4	24.7			
Gain (ha)		437.8	1478.3	130.2	0	1033.9	503.4	0			

Based on this study, about 83% of existing land may remain unchanged, particularly farmland (91%), settlement (84%) and plantation (78%). Conversely, only 10% of current natural vegetation cover would be unchanged, indicating a large amount of conversion to be occurred in the future.

An examination of LULC change over the study period highlighted substantial loss of natural and semi-natural landscape units and expansion of a human-dominated landscape. These changes have the potential to affect land productivity, habitat quality, ecological processes and functions, ecological resilience, and ultimately, general human well-being. Future land use management plans based on simulated LULC maps may prove important in reducing pressure on natural ecosystems and assist in minimizing the expansion of human land-use activities, thereby reducing or eliminating any further degradation of ecosystem functionality (Halmy et al., 2015).

3.3. Analysis of landscape composition and configuration

Five class-level metrics (LPI, MPS, AWMPFD, NP and AI) are selected following a stepwise analysis using both PCA (Table 9) and correlation analysis (Figure 9). The LPI and MPS (area metrics) are known as composition metrics, and the AWMPFD (shape metrics), NP and AI (aggregation metrics) represent landscape configurations.

3.3.1. Analysis of landscape structural changes in the Beressa watershed (1972–2017)

The temporal changes evident in the landscape pattern metrics for each LULC class are shown in Table 10. The LPI indicates how the patches resist fragmentation. The results reveal that LPI exhibits an increasing trend for farmland, plantation and settlement LULC, signifying where

dispersed patches were merged into larger areas. This signifies decreased fragmentation of the patches. Conversely, the LPI for natural vegetation (77.2%) and barren land (74.2%) is reduced, indicating increased human disturbance that resulted in widespread fragmentation. The LPI for grassland and waterbody covers exhibited an inconsistent, varied trend (Table 10), with grassland LPI was totally decrease by 79.4% and an increase for waterbody category by 77.2% during 1972–2017 (Figure 10).

High demand of firewood charcoal, and construction activities, and an increased demand for suitable cultivation areas were the main drivers for fragmentation of natural vegetation. Barren land and grassland patches were also fragmented due to increased demand of food for the growing population. A similar situation is identified in other Ethiopian highland areas (Gashaw et al., 2017; Yesuph and Dagnew, 2019).

The mean patch size (MPS) also showed a similar trend like LPI for farmland, plantation, settlement, natural vegetation, and waterbody, however a decreasing trend is observed for grassland and barren land (Table 10). The MPS for grassland and natural vegetation declined by 60% and 43.2% during 1972–2017 (Figure 10). It is a good indicator for understanding patch fragmentation. An increase of MPS can resulted from progressive clustering of patches (Liu et al., 2019) and an increase in patches size over time. A decreasing trend indicates the fragmentation of the patches.

Farmland recorded the largest LPI and MPS values, with the single largest farmland patch being 68.02% and the largest MPS being 92.94 h, both recorded in 2017 (Table 10). High LPI and MPS values are indicators of landscape homogeneity and the result clearly suggests the dominance of farmland in the watershed, this being the main socioeconomic, livelihood system of the local communities. This result is in line with Tolessa et al. (2016), who reported that the cultivated category

Table 9. Component pattern of rotated factor loadings.

Metrics	Principal components			Communalities
	1	2	3	
AWGYRATE	**0.99**[*]	-0.015	0.093	0.993
LPI	**0.99**	-0.018	0.068	0.989
AWMPS	**0.988**	-0.037	0.055	0.988
MESH	**0.982**	-0.048	0.048	0.979
DIVISION	**-0.982**	0.048	-0.048	0.98
PLAND	**0.972**	0.1	0.13	0.976
AWMPSI	**0.924**	0.119	0.087	0.945
AWMPFD	**0.892**	0.21	0.09	0.882
MPS	**0.798**	-0.19	0.063	0.901
ED	0.77	0.531	0.156	0.962
TE	0.769	0.531	0.156	0.962
IJI	0.519	-0.276	-0.293	0.652
PD	-0.169	**0.955**	0.025	0.942
NP	-0.169	**0.955**	0.025	0.942
LSI	0.269	**0.941**	0.075	0.985
MNENN	-0.235	-0.634	0.197	0.609
COHESION	0.332	0.075	**0.902**	0.932
AI	0.337	-0.191	**0.859**	0.91
SPLIT	-0.027	-0.16	**-0.846**	0.742
CONTIG	-0.38	-0.138	0.675	0.781
eigenvalue	10.89	4.53	2.73	
%variance	56.89	26.6	13.02	
%cumulative	56.87	83.5	96.51	

[*] Bold faced values are significant at $p < 0.05$.

forms large, contiguous patches in the Jibat forest of western highland Ethiopia. Muleta and Biru (2019) also concurred with this observation, reporting similar findings, and suggesting that expansion of cultivated land and settlement is primarily resulted from increased demand of food and shelters. On the other hand, waterbody and plantation categories display the smallest LPI (0.06%) and MPS (0.96 ha) (Table 10) in the study area.

The magnitude of change in plantation LPI (795.7%) and MPS (263.5%) was remarkably high during 1972–2017. Settlement category was next with a change rate in LPI of 231.3% and MPS was 134.4%. These high change rates indicate rapid expansion of plantation and settlement patches due to increased population pressure. Degraded areas of cultivated lands were converted to plantation patches, while high demand and market value of firewood resulted in the expansion of *Eucalyptus* plantations into fertile and productive lands. This indicates that *Eucalyptus* plantations are also expanding in the area at the expense of crop production due to increased cash flow from these products, resistance of the tree species to pests and diseases, and the associated low maintenance and labour costs. Others have also reported similar findings in the Koga and Mega watersheds of Ethiopia (Chanie et al., 2013; Negasa et al., 2016).

One of the main reasons for settlement patch augmentation was land reallocation for young couples and retired military personnel (Yesuph and Dagnew, 2019). Socio-economic development and industrial growth have resulted in a progressive expansion of urban and industrial areas (e.g. industrialization in and around Debre Berhan town). This has resulted in an increase in development in the lower sections of the watershed, usually at the expense of existing agricultural areas. The urban ecosystem tends to be more complex, including social-biophysical feedback with intense human influences. Urban systems alter air and soil quality and lead to significant loss of biodiversity (with small patches less likely to support a wide variety of habitats and species) due to increased human habitation, construction of artificial structures and loss of natural

habitat (Parris, 2018; Walt et al., 2015). On the contrary, the lowest LPI change was observed in farmland (increased by 47.5%) and in waterbody for MPS (decreased by 1%) during the study period (Figure 10). The low change rate in farmland attributed to relatively slow expansion as compared to others such as farmland which was covered more than half of the watershed before 1972.

The loss of area and habitat fragmentation increased for natural vegetation, grassland, and barren land covers as indicated with a rapid decline of LPI and MPS during 1972–2017 (Figure 10). With the landscape increasingly fragmented, average size of the patches has decreased (Wu, 2009). Class-level loss and fragmentation have occurred as the watershed is experiencing a continued loss of natural vegetation, grassland and barren land. Amsalu et al. (2007) observed the same issue in the study area, noting continuous clearing of natural vegetation since 1950s. Many other studies conducted in Ethiopia have noted that ongoing deforestation is a major cause of land degradation (Duguma et al., 2019).

In terms of NP, plantation is the patchiest category (Table 10). The NP increased continually for barren land with a total change rate of 69.7%, settlement by 65.8%, and grassland by 28.6%. An increase in the grassland and barren land patches indicated that they are under severe anthropogenic pressure. This finding corroborates with other studies in Ethiopia and elsewhere (Amsalu et al., 2007; Meshesha et al., 2016; Tolessa et al., 2016; Walt et al., 2015). The expansion of settlement leads to the changes in composition and functioning of adjacent lands through disturbance impacts (Walt et al., 2015). As a result, grassland cover adjacent to urban areas in the lower part of the watershed become highly susceptible to fragmentation.

The NP for natural vegetation, waterbody, plantation and farmland has varied since 1972. For example, the NP for natural vegetation and waterbody increased from 1972 to 1987, but decreased from 1987 to 2017 (Table 10), with a decline rate of 53.1% and 33.9%, respectively during 1972–2017 (Figure 10). This decreasing trend implies that there was a substantial loss of these classes due to increased human
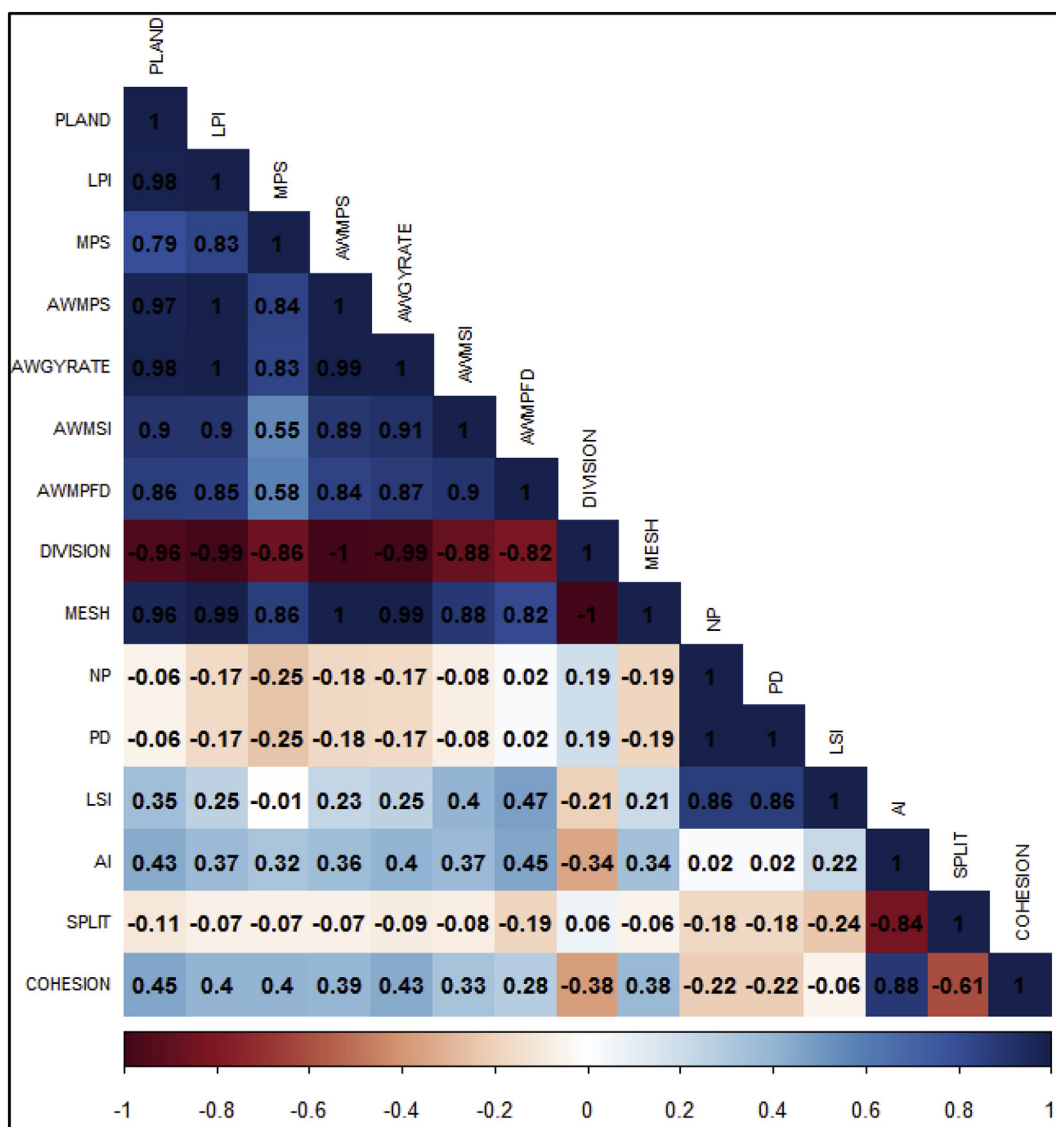
Figure 9. Spearman's rank correlation heat map between landscape metrics. Dark blue color indicates strong positive relationships, dark red indicates strong negative relationship.

interference and high demand for fuelwood. A rapid growth in plantation patches (171.4%) was recorded, although NP did decrease from 886 to 836 between 2002 and 2017. The NP for farmland showed a consistent increase between 1972 and 2002, and then a decrease from 2002 to 2017. The increasing trend noted was due to frequent land redistribution in the area, while decreasing trend indicated that farmland patches merged together to form larger patches (as evidenced by the MPS and LPI trend). Tolessa et al. (2016) noted that cultivated land NP increased due to the fact that farmers owned many parcels in Jibat forest, Ethiopia.

The AI of the patches were above the medium value (60.6%). During 1972–2017, all LULC covers experienced this decreased except for farmland and waterbody covers (Table 10). A decrease in AI, together with an escalation of NP for the settlement and plantation categories is attributed to spontaneous growth of the patches (Hao et al., 2012; Parris, 2018). As NP increased, a decline in AI, MPS and LPI for natural vegetation and grassland patches was noted, suggesting fragmentation of lands.

The analysis of AWMPFD indicates that, generally, most of the patches shape are less complex (Table 10). This could be the result of the landscape having uniform patch boundaries due to human activities (Saura and Carballal, 2004). The simplest patch shape observed in

settlement and plantation was 1.09, while relatively more irregular patch shapes were observed in the farmland category (1.37). Overall, the shape complexity increased for farmland, grassland, plantation and settlement covers, while it decreased for the barren land, natural vegetation and waterbody categories. The change of shape irregularity was highest for grassland (11.5%) and lowest for waterbody (0.9%) during 1972–2017.

3.3.2. Landscape structural changes for simulated land use/land cover

The landscape metrics assessment for projected LULC revealed that LPI and MPS would increase for plantation (404.3% and 92.7% respectively), settlement (120% and 298.8%) barren land (230.3% and 59.1%) and farmland (2.4% and 25%). However, they could decrease for natural vegetation (97.3% and 63.9%) and waterbody (27.3% and 73.7%) covers during 2017–2047 (Figure 10). The LPI and MPS of grassland cover could fluctuate during 2017–2047, with an increase of LPI and a corresponding decrease in MPS from 2017 to 2032. They did, however, showed a reversed tendency from 2032 to 2047 (Table 10). In total, LPI and MPS for grassland could decrease by 35% and 30.8% during 2017–2047. The greatest changes in LPI and MPS are expected to be for plantation and settlement categories, and the least change could be for farmland cover. Despite having the least change, the LPI and MPS for farmland will

Table 10. Observed and predicted landscape pattern metrics for each LULC.

Land use class	Year	Landscape metrics				
		LPI	MPS	AWMPFD	NP	AI
Barren land	1972	1.28	6.77	1.17	346	84.61
	1987	1.18	1.35	1.15	384	82.2
	2002	0.39	4.08	1.14	454	77.61
	2017	0.33	1.54	1.13	587	70.81
	2032	0.43	2.26	1.08	210	89.39
	2047	0.44	2.20	1.08	108	89.92
Farmland	1972	46.13	41.42	1.32	296	91.55
	1987	64.39	51.28	1.33	297	61.56
	2002	66.04	52.23	1.37	309	90.34
	2017	68.02	92.94	1.37	159	91.62
	2032	68.66	106.06	1.29	150	96.11
	2047	69.63	116.22	1.27	142	97.09
Grassland	1972	3.78	9.28	1.13	304	86.61
	1987	3.01	6.50	1.19	313	84.2
	2002	3.73	5.03	1.2	365	82.32
	2017	0.78	3.71	1.26	391	81.42
	2032	0.83	3.50	1.09	172	82.61
	2047	0.51	2.57	1.08	149	83.67
Natural vegetation	1972	1.62	5.93	1.15	245	81.72
	1987	1.26	4.47	1.13	258	80.55
	2002	0.95	3.37	1.14	148	80.28
	2017	0.37	3.37	1.12	115	79.42
	2032	0.12	2.60	1.11	113	81.38
	2047	0.01	1.22	1.05	105	82.29
Plantation	1972	0.23	0.96	1.09	308	77.43
	1987	0.35	1.86	1.11	379	74.68
	2002	0.78	2.89	1.15	886	70.31
	2017	2.06	3.49	1.18	836	69.34
	2032	3.91	15.52	1.1	332	80.34
	2047	3.97	17.59	1.1	373	82.71
Settlement	1972	0.32	1.21	1.09	322	89.32
	1987	0.42	1.92	1.12	332	82.02
	2002	0.78	2.11	1.13	443	80.06
	2017	1.06	2.83	1.13	534	77.08
	2032	1.48	9.79	1.04	382	81.48
	2047	2.33	11.28	1.06	367	84.74
Waterbody	1972	0.07	9.45	1.16	56	64.01
	1987	0.07	6.83	1.16	57	61.56
	2002	0.06	3.53	1.19	43	60.6
	2017	0.11	9.36	1.15	37	81.1
	2032	0.09	3.04	1.07	29	87.01
	2047	0.08	2.46	1.07	25	88.74

become very large (69.63% and 116.22 ha) relative to the other categories (Table 10).

The NP may decline for all LULC patches with the exception of a slight increase in plantation cover from 2032 to 2047. The decline of NP could be highest for barren land (81.6%) and lowest for natural vegetation (8.7%) during 2017–2047. The NP may decline due to the possible merging of similar patches. A decline of NP and corresponding increase in MPS and LPI indicates a convergence of patches, typical for farmland, plantation, settlement, and barren land. This is evidenced by an increase in patches aggregation. The settlement patch could assemble together to form villages and towns as shown by Tolessa et al. (2016). As de Groot (2006) explained, different human activities result in the conversion of multi-functional landscapes into more homogenous human-dominated landscapes.

Over the projected period, the landscape becomes more contiguous as AI would increase for all classes with the highest aggregation could be for

farmland (97.09%) and lowest aggregation of might be for plantation (80.34%) (Table 10). The patches of plantation become progressively aggregated and the change rate can be highest (19.3%) whereas grassland patches may be aggregated gradually (2.8%) (Figure 10). This may be a consequence of a decrease in NP and a concomitant increase in MPS.

In the future, the shape of all land class patches is expected to be simpler. Human-modified landscape patches may experience overall simpler shapes (Saura and Carballal, 2004; Uuemaa et al., 2011. Relative shape complexity is expected to decrease consistently for farmland, grassland, and natural vegetation. The AWMPFD for plantation, barren land and waterbody is likely to decrease between 2017 and 2032 but may be unchanged from 2032 to 2047. Analysis of settlement category (with the least patch shape complexity), indicated a decrease between 2017 and 2047 and a slight increase from 2032 to 2047 (Table 10). The greatest decline of AWMPFD is expected for grassland category (14.3%), and the least change is expected to be for barren land (4.4%) (Figure 10).
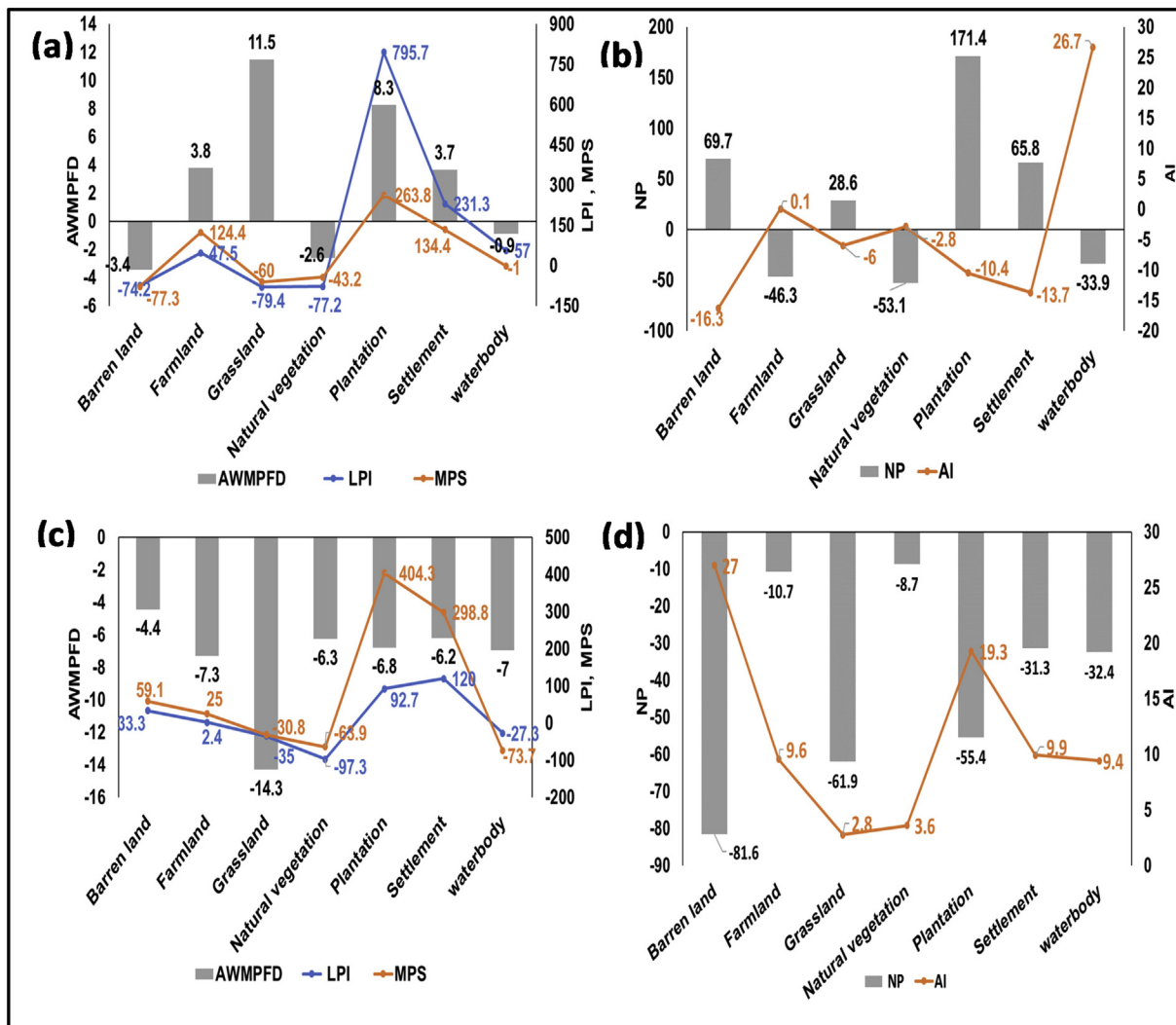
Figure 10. Changes in landscape metrics during 1972–2017 (a–b); and 2017–2047 (c–d).

In general, ongoing landscape structural change can have negative implications for ecological functions, processes which could result in reduced ecosystem services (Pazurova et al., 2018). For example, the landscape of the Beressa watershed can progressively be exposed to high runoff, sedimentation, soil degradation and resource depletion, and subsequent reduction in crop yield (Worku et al., 2017; Amsalu et al., 2007). Negative consequences resulting from this landscape structural changes may accelerate in the future, if appropriate strategies are not developed.

4. Conclusion

The objective of this paper was to evaluate current and projected landscape structural changes in a region of Ethiopia. LULC transition matrix and landscape metrics of LPI, MPS, AWMPFD, NP and AI were used to identify these changes. Results revealed that landscape of the Beressa watershed has experienced profound structural change since 1972. The landscape has become human-dominated as a result of rapid LULC change. The natural and semi-natural land covers, namely natural vegetation, grassland, waterbody, and barren land, have reduced. Farmland is currently the predominant LULC with spatially less isolated patches. Farmland also has the largest LPI and MPS and highest AI and shows consistent growth in both past and future periods. Plantation and settlement patches have also expanded and exhibited a pattern of simpler patch shapes which are expected to be aggregated over time. A

consistent increase in farmland, plantation, and settlement categories is indicative of increasing food demand from a fast-growing population. Farmland and plantations have also increasingly expanded into areas of steeper slopes and more marginal soil profiles. At the same time, natural vegetation and waterbody categories have declined and become more fragmented. Grassland and barren land have also declined and become more fragmented as the number of patches has increased. It is expected that these declining trends will continue into the future as the patches become more compact. Observed landscape structural change, a result of large-scale ongoing modifications to LULC, has several environmental and socio-economic implications, including a decline in land productivity, loss of biodiversity loss, all of which are detrimental to long-term environmental sustainability. As ecological processes are dependent on landscape structure, further research in the area of landscape structure and landscape processes, functions, and services, is warranted.

Declarations

Author contribution statement

Hamere Yohannes: Conceived and designed the experiments; Performed the experiments; Analyzed and interpreted the data; Contributed reagents, materials, analysis tools or data; Wrote the paper.

Teshome Soromessa: Conceived and designed the experiments; Performed the experiments; Contributed reagents, materials, analysis tools or data; Wrote the paper.

Mekuria Argaw: Performed the experiments; Contributed reagents, materials, analysis tools or data; Wrote the paper.

Ashraf Dewan: Performed the experiments; Contributed reagents, materials, analysis tools or data; Wrote the paper.

Competing interest statement

The authors declare no conflict of interest.

Additional information

No additional information is available for this paper.

References

Alharbi, O.M.L., Arsh, A., Khattab, R.A., Ali, I., 2018. Health and environmental effects of persistent organic pollutants. J. Mol. Liq. 263 (May).

Ali, I., Al-othman, Z.A., Abdulrahman, A., 2015. Removal of secbumeton herbicide from water on composite nanoadsorbent. Desalination and Water Treatment 37–41.

Ali, I., Gupta, V.K., Aboul-Enein, H.Y., 2005. Metal ion speciation and capillary electrophoresis: application in the new millennium. Electrophoresis 26, 3988–4002.

Alia, I., Alwarthan, Z.A.A.A., 2017. Supra molecular mechanism of the removal of 17-β-estradiol endocrine disturbing pollutant from water on functionalized iron nano particles. J. Mol. Liq. 241, 123–129.

Amsalu, A., Stroosnijder, L., Graaff, J. De., 2007. Long-term dynamics in land resource use and the driving forces in the Beressa watershed, highlands of Ethiopia. J. Environ. Manag. 83, 448–459.

Apan, A.A., Raine, S.R., Paterson, M.S., 2002. Mapping and analysis of changes in the riparian landscape structure of the Lockyer Valley catchment, Queensland, Australia. Landsc. Urban Plann. 59, 43–57.

Araya, Y.H., Cabral, P., 2010. Analysis and modeling of urban land cover change in setúbal and sesimbra, Portugal. Rem. Sens. 2, 1549–1563.

Basheer, A.A., 2017. Chemical chiral pollution: impact on the society and science and need of the regulations in the 21 st century. Chirality (October), 1–5.

Basheer, A.A., Ali, I., 2018. Stereoselective uptake and degradation of (±) - o, p - DDD pesticide stereomers in water - sediment system. Chirality (April), 1–8.

Berihun, M.L., Tsunekawa, A., Haregeweyn, N., Meshesha, D.T., Adgo, E., Thubo, M., Yiberltal, M., 2019. Exploring land use/land cover changes, drivers and their implications in contrasting agro-ecological environments of Ethiopia. Land Use Pol. 87, 104052.

Burakova, E.A., Dyachkova, T.P., Rukhov, A.V., Tugolukov, E.N., Galunin, E.V., Tkachev, A.G., Ali, I., 2018. Novel and economic method of carbon nanotubes synthesis on a nickel magnesium oxide catalyst using microwave radiation. J. Mol. Liq. 253, 340–346.

Cat Tuong, T.T., Tani, H., Wang, X., Thang, N.Q., 2019. Semi-supervised classification and landscape metrics for mapping and spatial pattern change analysis of tropical forest types in thua thien hue province, vietnam. Forests 10 (8), 673.

Chanie, T., Collick, A.S., Adgo, E., Lehmann, C.J., Steenhuis, T.S., 2013. Eco-hydrological impacts of Eucalyptus in the semi humid Ethiopian highlands: the lake tana plain. J.Hydrol. Hydromech 61 (1), 21–29.

Chu, L., Sun, T., Wang, T., Li, Z., Cai, C., 2018. Evolution and prediction of landscape pattern and habitat quality based on CA-markov and InVEST model in hubei section of three gorges reservoir area (TGRA). Sustainability 10, 3854.

Congalton, Russel G., Green, K., 2009. Assessing the Accuracy of Remotely Sensed Data: Principles and Practices, second ed. Taylor & Francis Group, Boca Raton, London.

Congedo, L., 2016. Semi-Automatic Classification Plugin User Manual.

Cushman, S.A., Mcgarigal, K., Neel, M.C., 2008. Parsimony in landscape metrics: strength, universality, and consistency. Ecol. Indicat. 8, 691–703.

Daley, B., 2015. Environmental Issues in Ethiopia and Links to the Ethiopian Economy, Evidence on Demand.

Daye, D.D., 2012. Fragmented Forests in South-West Ethiopia: Impacts of Land- Use Change on Plant Species Composition and Priorities for Future Conservation. PhD Dissertation. Bangor University, Bangor, United Kingdom.

de Groot, R., 2006. Function-analysis and valuation as a tool to assess land use conflicts in planning for sustainable, multi-functional landscapes. Landsc. Urban Plann. 75, 175–186.

Dewan, A.M., Yamaguchi, Y., Rahman, Z., 2012. Dynamics of land use/cover changes and the analysis of landscape fragmentation in Dhaka Metropolitan, Bangladesh. Geojournal 77 (3), 315–330.

Dezhkam, S., Amiri, B.J., Darvishsefat, A.A., Sakieh, Y., 2017. Performance evaluation of land change simulation models using landscape metrics. Geocarto Int. 32 (6), 655–677.

Duguma, L.A., Atela, J., Minang, P.A., Ayana, A.N., Gizachew, B., Nzyoka, J.M., Bernard, F., 2019. Deforestation and forest degradation as an environmental behavior: unpacking realities shaping community actions. Land 8 (26), 1–17.

Dunlap, R.E., Jorgenson, A., 2012. Environmental problems. In: The Wiley-Blackwell Encyclopedia of Globalization.

Eastman, J.R., 2012. IDRISI Selva Tutorial Manual Version 17.01. Clark University, Worcester.

EMA (Ethiopia Meteorology Agency), 2017. Weather Data of Beressa Watershed from Debre Berhan and Debele Stations from 1986 to 2017.

Fenta, A.A., Yasuda, H., Haregeweyn, N., Belay, S., Hadush, Z., Gebremedhin, M.A., Mekonnen, G., 2017. The dynamics of urban expansion and land use/land cover changes using remote sensing and spatial metrics: the case of Mekelle City of northern Ethiopia. Int. J. Rem. Sens. 38 (14), 4107–4129.

Gashaw, T., Tulu, T., Argaw, M., Worqlul, A.W., 2017. Evaluation and prediction of land use/land cover changes in the Andassa watershed, Blue Nile Basin, Ethiopia. Environmental Systems Research 6 (17).

Gelet, M., Suryabhagavan, K., Balakrishnan, M., 2010. Land-use and landscape pattern changes in holeta-berga water shed, Ethiopia. Int. J. Ecol. Environ. Sci. 36 (2–3), 117–132.

Halmy, W.M.A., Gessler, P.E., Hicke, J.A., Salem, B.B., 2015. Land use/land cover change detection and prediction in the north-western coastal desert of Egypt using Markov-CA. Appl. Geogr. 63, 101–112.

Hamza, I., Iyela, A., 2012. Land use pattern, climate change, and its implication for food security in Ethiopia: a Review. Ethiopian Journal of Environmental Studies and Management 5 (1), 26–31.

Hao, R., Su, W., Yu, D., 2012. Quantifying the type of urban sprawl and dynamic changes in shenzhen. In: Computer and Computing Technology in Agriculture (CCTA), sixth ed., pp. 407–415.

Hassan, Z., Shabbir, R., Ahmad, S.S., Malik, A.H., Aziz, N., Butt, A., 2016. Dynamics of land use and land cover change (LULCC) using geospatial techniques: a case study of Islamabad Pakistan. SpringerPlus 5 (812).

Jayne, T.S., Chamberlin, J., Headey, D.D., 2014. Land pressures, the evolution of farming systems, and development strategies in Africa: a synthesis. Food Pol. 48, 1–17.

Kindu, M., Schneider, T., Teketay, D., Knoke, T., 2013. Land use/land cover change analysis using object-based classification approach in munessa-shashemene landscape of. Rem. Sens. 5, 2411–2435.

Kumar, M., Denis, D.M., Kumar, S., Szabó, S., Suryavanshi, S., 2018. Landscape metrics for assessment of land cover change and fragmentation of a heterogeneous watershed. Remote Sensing Applications: Society and Environment 10, 224–233.

Lillesand, R., Kiefer, R.W., 1999. Remote Sensing and Image Interpretation, fourth ed. John Willy & Sons Inc. 1999.

Liu, H., Weng, Q., 2013. Landscape metrics for analysing urbanization-induced land use and land cover changes. Geocarto Int.

Liu, S., Yu, Q., Wei, C., 2019. Spatial-temporal dynamic analysis of land use and landscape pattern in guangzhou, China: exploring the driving forces from an urban sustainability perspective. Sustainability 11 (6675).

Macchi, S., Tiepolo, M., 2014. Urban sprawl as a factor of vulnerability to climate change: monitoring land cover change in dar es salaam. In: John Dodson, A., Menai (Eds.), Climate Change Vulnerability in Southern African Cities. Spronger Climate, pp. 73–88.

Matsushita, B., Xu, M., Fukushima, T., 2006. Characterizing the changes in landscape structure in the Lake Kasumigaura Basin, Japan using a high-quality GIS dataset. Landsc. Urban Plann. 78, 241–250.

McGarigal, K., Cushman, S., Neel, M., Ene, E., 2012. FRAGSTATS V4: Spatial Pattern Analysis Program for Categorical and Continuous Maps. Computer Software Program Produced by the Authors at the University of Massachusetts, Amherst. http://www.umass.edu/landeco/research/fragstats/fragstats.html. Retrieved from.

Meshesha, W.T., Tripathi, M.S.K., Khare, D., 2016. Analyses of land use and land cover change dynamics using GIS and remote sensing during 1984 and 2015 in the Beressa Watershed Northern Central Highland of Ethiopia. Modeling Earth Systems and Environment 2 (4), 1–12.

Minta, M., Kibret, K., Thorne, P., Nigussie, T., Nigatu, L., 2018. Land use and land cover dynamics in Dendi-Jeldu hilly-mountainous areas in the central Ethiopian highlands. Geoderma 314, 27–36.

Mohamed, A., Worku, H., 2020. Urban Climate Simulating urban land use and cover dynamics using cellular automata and Markov chain approach in Addis Ababa and the surrounding. Urban Climate 31 (May 2019), 100545.

Mohamed, A., Worku, H., Kindu, M., 2019. Quantification and mapping of the spatial landscape pattern and its planning and management implications a case study in Addis Ababa and the surrounding area, Ethiopia. Geology, Ecology, and Landscapes 1, 1–12.

Mohd, I.A., Khan, A.T.A., 2013. Arsenite removal from water by electro-coagulation on zinc – zinc and copper – copper electrodes. Int. J. Environ. Sci. Technol. 10, 377–384.

MoWIE, 2017. Ethiopia Ministry of Water Irrigation and Electricity. GIS data of Amhara region.

Munthali, M.G., Davis, N., Adeola, A.M., Botai, J.O., Kamwi, J.M., Chisale, H.L.W., Orimoogunje, O.O.I., 2019. Local perception of drivers of land-use and land-cover change dynamics across dedza district, Central Malawi region. Sustainability 11 (832).

Muleta, Terefe T., Biru, Moges K., 2019. Human modified landscape structure and its implicationon ecosystem services at Guder watershed in Ethiopia. Environ. Monit. Assess 191 (295).

Nagendra, H., Munroe, D.K., Southworth, J., 2004. From pattern to process: landscape fragmentation and the analysis of land use/land cover change. Agric. Ecosyst. Environ. 101, 111–115.

Negasa, D.J., Mbilinyi, B., Mahoo, H., Lemenih, M., 2016. Evaluation of land use/land cover changes and Eucalyptus expansion in meja evaluation of land use/land cover changes and Eucalyptus expansion in meja watershed, Ethiopia. Journal of Geography, Environment and Earth Science International 7 (3), 1–12.

Nurwanda, A., Fitriany, A., Zain, M., Rustiadi, E., 2016. Analysis of land cover changes and landscape fragmentation in Batanghari Regency, Jambi Province. Procedia - Social and Behavioral Sciences 227, 87–94.

Palmate, S.S., Pandey, A., Mishra, S.K., 2017. Modelling spatiotemporal land dynamics for a trans-boundary river basin using integrated Cellular Automata and Markov chain approach. Appl. Geogr. 82, 11–23.

Parris, K.M., 2018. Existing ecological theory applies to urban environments. Landsc. Ecol. Eng. 14 (2), 201–208.

Pazurova, Z., Pouwels, R., Bolliger, J., 2018. Effects of landscape changes on species viability: a case study from northern Slovakia. Sustainability 10 (3602).

Pontius Jr., R.G., Millones, M., 2011. Death to Kappa: birth of quantity disagreement and allocation disagreement for accuracy assessment. Int. J. Rem. Sens. 32 (15), 4407–4429.

Prokopov, M., Salvati, L., Egidi, G., Cudlín, O., Vcelakova, R., Plch, R., Cudlín, P., 2019. Envisioning present and future land-use change under varying ecological regimes and their influence on landscape stability. Sustainability 11 (4654).

Riitters, K.H., Neil, R.V.O., Hunsaker, C.T., Wickham, J.D., Yankee, D.H., Timmins, S.P., 1995. A factor analysis of landscape pattern and structure metrics. Landsc. Ecol. 10 (1), 23–39.

Rudel, T.K., 2009. Tropical deforestation how do people transform landscapes? A sociological perspective on suburban sprawl and tropical deforestation. Am. J. Sociol. 115 (1), 129–154.

Rujoiu-Mare, M.-R., Mihai, B., 2016. Mapping land cover using remote sensing data and gis techniques: a case study of prahova subcarpathians. Procedia Environmental Sciences 32, 244–255.

Saura, S., Carballal, P., 2004. Discrimination of native and exotic forest patterns through shape irregularity indices: an analysis in the landscapes of Galicia, Spain. Landsc. Ecol. 19, 647–662.

Singh, Sudhir Kumar, Mustak, S.k., Srivastava, Prashant K., Szabó, Szilárd, Islam, Tanvir, 2015. Predicting spatial and decadal LULC changes through cellular automata markov chain models using earth observation datasets and geo-information. Environ. Process 2, 61–78.

Tolessa, T., Senbeta, F., Kidane, M., 2016. Landscape composition and configuration in the central highlands of Ethiopia. Ecology and Evolution 6, 7409–7421.

Uuemaa, Evelyn, Roosaare, Jüri, Oja, Tõnu, Mander, Ülo, 2011. Analysing the spatial structure of the Estonian landscapes: which landscape metrics are the most suitable for comparing different landscapes? Estonian J. Ecol. 60 (1), 70–80.

Vadjunec, J.M., Frazier, A.E., Kedron, P., Fagin, T., Zhao, Y., 2018. A land systems science framework for bridging land system Architecture and landscape ecology: a case study from the southern high plains. Land 7 (27).

Walt, L. Van Der, Cilliers, S.S., Kellner, K., Toit, M. J. Du, Tongway, D., 2015. To what extent does urbanization affect fragmented grassland functioning? J. Environ. Manag. 151, 517–530.

Weide, A.C., Beauducel, A., 2019. Varimax rotation based on gradient projection is a feasible alternative to SPSS. Front. Psychol. 10, 1–14.

Worku, T., Khare, D., Tripathi, S.K., 2017. Modeling runoff – sediment response to land use/land cover changes using integrated GIS and SWAT model in the Beressa wat. Environmental Earth Sciences 76 (550).

Wu, J., 2009. Ecological dynamics in fragmented landscapes. In: Princeton Guide to Ecology (In: Simon. Princeton University Press, pp. 438–444.

Yang, X., Zheng, X., Chen, R., 2014. A land use change model: integrating landscape pattern indexes and Markov-CA. Ecol. Model. 283, 1–7.

Yesuph, A.Y., Dagnew, A.B., 2019. Land use/cover spatiotemporal dynamics, driving forces and implications at the Beshillo catchment of the Blue Nile Basin, North Eastern Highlands of Ethiopia. Environmental Systems Research 8 (21).

Zhang, F., Li, Y., Liu, S., Zhao, S., Wu, Y., 2014. Dynamic monitoring of landscape patterns and ecological processes using HJ-1 and SPOT satellite data over Hulunbeier grassland, China. J. Earth Syst. Sci. 123 (2), 319–328.